

INTERACTING CRACKS AND INCLUSIONS IN A SOLID BY MULTIPOLE EXPANSION METHOD

V. I. KUSHCH

Institute for Superhard Materials, National Academy of Sciences of Ukraine, 2,
Avtozavodskaya Str., 254074 Kiev, Ukraine
E-mail: frd@ismanu.kiev.ua

(Received 12 November 1996; in revised form 11 May 1997)

Abstract—An accurate series solution is obtained of the elastic problem for a solid containing penny-shaped cracks and spheroidal inclusions or cavities. The method of solution is based on the general solution procedure developed by Kushch [(1996) *Elastic equilibrium of a solid containing a finite number of aligned inclusions. International Journal of Solids and Structures* 33, 1175–1189] and consists in representation of the displacement vector by a series of the vectorial partial solutions of Lamé's equation, written in a spheroidal basis. By using the addition theorems for these partial solutions the primary boundary-value problem is reduced to an infinite set of linear algebraic equations. An asymptotic analysis of the problem is performed and the series expansion of the opening-mode stress intensity factor is obtained. Numerical analysis of model problems is performed and some results demonstrating the effect on the stress intensity factor of the pair interactions in crack–crack, crack–cavity and crack–inclusion geometries are presented. © 1998 Elsevier Science Ltd.

1. INTRODUCTION

The majority of composite materials contain, besides the reinforcing phase, structural inhomogeneities of other kinds. The most commonly occurring structure defects are cracks, that can arise during the time the composite is manufactured or utilised. Their presence under certain conditions may lead to a significant decrease in the mechanical properties and strength of the composite. To understand more deeply the nature of this phenomenon, we should determine how a crack interacts on a micro level with other cracks and with particles of disperse phase. Such knowledge is necessary if we want to develop a reliable theory of strength of composites with imperfect phases. It also provides the theoretical background for development of composites with advanced properties. Thus, the problem stated in the article's title is of both theoretical and practical interest.

It should be noted, however, that serious mathematical difficulties arise when we try to consider a problem for the interaction of cracks and inclusions in a solid in three dimensions. Unlike the two-dimensional case, where powerful techniques, e.g. the method of Kolosov–Muskhelishvili's complex potentials, are well-established and work successfully, for spatial elasticity problems until now there are no analogous methods to solve a wide class of problems of elasticity theory in multiply-connected domains. Due to this reason, a relatively small number of publications can be found from the open literature where problems of this kind are treated.

The application of mathematical methods to analyse three-dimensional crack problems was pioneered by Sack (1946) and Sneddon (1946) who solved the problem for a single penny-shaped crack in an infinite elastic medium. The problem becomes much more complicated when two or more interacting cracks in a solid are considered. Various approaches were developed to solve problems of this kind. The most frequently used idea is the formulation of the crack problem as a problem in potential theory. So, to solve the problem for two coplanar penny-shaped cracks this approach was used by Collins (1963) for a normal type loading and by Fu and Keer (1969) for a shear loading. More recently the problem of a finite sized domain containing a finite number of arbitrarily spaced and oriented cracks was studied by Andrejiv (1982) and by Kit and Hay (1989). In all these works the potential theory problem was reduced to an infinite set of Fredholm integral

equations of the second kind. This is a difficult mathematical problem in itself. In the special case, when the distance between the cracks is sufficiently large compared with their radii, the approximate solution of the integral equations can be found by iteration (Collins, 1963).

Another way was chosen by Sneddon (1966) who used the Kobayashi potentials and the addition theorems for Bessel's functions to reduce the potential theory problem to an infinite set of simultaneous algebraic equations. An attempt to combine the superposition principle of elasticity theory with Eshelby's equivalent inclusion method to study the problem for two penny-shaped cracks was taken by Xiao *et al.* (1994). We point out also the paper by O'Donaghue *et al.* (1985) where a finite-element analysis of interacting elliptic cracks was performed. To the author's knowledge, the three-dimensional problem on the interacting crack and inclusion has never been considered; all the sources cited above deal with interacting cracks only.

An accurate solution of the linear elastostatics problem for a solid containing a finite number of aligned spheroidal inclusions was obtained by Kushch (1996). In the context of composite mechanics this problem can be treated as a many-particle model of composite. Unlike the commonly used one-particle model (space with a single inclusion), such a model provides taking into account arrangement and interactions of the particles of disperse phase. The essence of the method of solution developed is the representation of the displacement vector in each subdomain by a series of the partial vectorial solutions of Lamé's equation written in a spheroidal basis. The superposition principle is utilised to build up the general solution in a multiply-connected (matrix) domain. To satisfy exactly all the interface conditions, the addition theorems for the above mentioned vectorial partial solutions are used. As a result, the primary boundary-value problem is reduced to an infinite set of linear algebraic equations that can be solved effectively. Recently this approach was extended by Kushch (1998) to the case of arbitrary oriented spheroidal inclusions or cavities.

Now we make use of the fact that the penny-shaped crack can be considered as the limiting case of the oblate spheroidal cavity when its smaller semi-axis tends to zero. Therefore, the problem for interacting cracks and inclusions in a solid can be studied within the framework of the aforementioned approach. Additional efforts are needed, however, in order to evaluate the stressed state in the vicinity of the crack's boundary where some components of the stress tensor tend to infinity. An analysis of this problem and calculation of the stress intensity factor for the crack, interacting with other cracks or inclusions, is the main subject of the paper. First, we introduce the basic notations and outline in brief the solution procedure.

2. GENERAL FORM OF THE SOLUTION FOR A MANY-PARTICLE MODEL

According to the general scheme of the superposition principle, the displacement vector in an unbounded solid containing a finite number N of spheroidal cavities or inclusions (Fig. 1) can be represented in the form

$$\mathbf{u}^{(0)} = \mathbf{U}_0 + \sum_{p=1}^N \mathbf{U}_p. \quad (1)$$

The first term in eqn (1) \mathbf{U}_0 is a regular part of the solution describing the far field and the second term is a superposition of the disturbance fields \mathbf{U}_p , produced by the inhomogeneities. Because \mathbf{U}_0 is limited in any point of the domain, it can be expanded into a series of the regular, or internal, partial solutions of Lamé's equation. On the contrary, the series expansion of the disturbance field \mathbf{U}_p , disappearing at infinity, contains the singular, or external, partial solutions only. Thus,

$$\mathbf{U}_0 = \sum_{i=1}^3 \sum_{l=0}^{\infty} \sum_{s=-l}^l a_{is}^{(i)} \mathbf{s}_{is}^{(i)}(\mathbf{r}_1, f_1), \quad \mathbf{U}_p = \sum_{i=1}^3 \sum_{l=0}^{\infty} \sum_{s=-l}^l A_{is}^{(i)(p)} \mathbf{S}_{is}^{(i)}(\mathbf{r}_p, f_p) \quad (2)$$

where $a_{is}^{(i)}$ and $A_{is}^{(i)(p)}$ are the constant series coefficients and $\mathbf{s}_{is}^{(i)}$ and $\mathbf{S}_{is}^{(i)}$ are the internal and

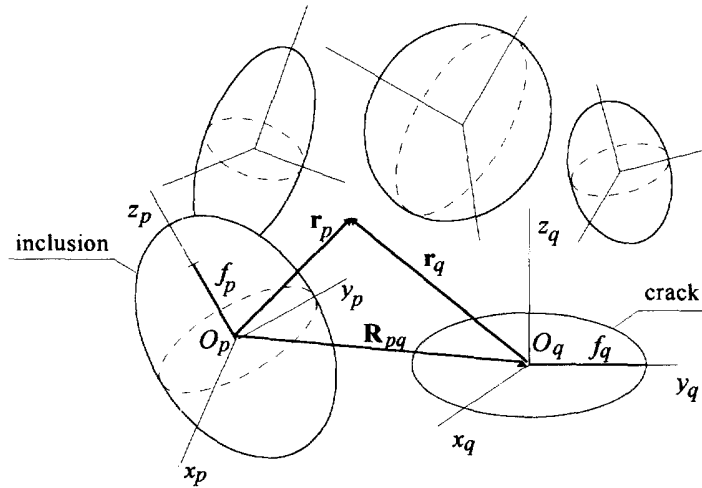


Fig. 1. Many-particle model of a composite.

external partial vectorial solutions, respectively, of Lamé’s equation written in the spheroidal coordinates (f, ξ, η, ϕ) , where f is a focal parameter (one-half of inter-foci distance). For the explicit form of the functions $\mathbf{s}_{is}^{(i)}$ and $\mathbf{S}_{is}^{(i)}$ [see Kushch (1996, 1998)]. Note, that in the series expansion (2) of \mathbf{U}_p the functions $\mathbf{S}_{is}^{(i)}$ are written in the p th local coordinate basis (x_p, y_p, z_p) with the radius-vector \mathbf{r}_p introduced so that an origin O_p of the coordinate system coincides with the centre of the p th inclusion and the $O_p z_p$ axis is the rotation axis of this spheroid as well. The local spheroidal coordinates $(f_p, \xi_p, \eta_p, \phi_p)$ are chosen so that the coordinate surface $\xi_p = \xi_p^{(0)}$ coincides with the surface of the p th inhomogeneity. They are related to the local Cartesian coordinates (x_p, y_p, z_p) by the known formulae

$$x_p + iy_p = f_p \xi_p \bar{\eta}_p \exp(i\phi_p), \quad z_p = f_p \bar{\xi}_p \eta_p;$$

where

$$\bar{\xi}_p = \sqrt{(\xi_p)^2 - 1}, \quad \bar{\eta}_p = \sqrt{1 - (\eta_p)^2}; \quad \xi_p \geq 1, \quad |\eta_p| \leq 1, \quad 0 \leq \phi_p < 2\pi.$$

The relations (2) are written for the case of an oblate spheroid which is of particular interest for us. For $\xi_p^{(0)} \rightarrow 1$ ($\bar{\xi}_p^{(0)} \rightarrow 0$) the surface $\xi_p = \xi_p^{(0)}$ of a spheroidal cavity tends to a penny-shaped crack of radius f_p . It is fairly straightforward to show that all the theory developed by Kushch (1996, 1998) is applicable without any limitations in the case of an infinitely thin oblate spheroid.

So, let us consider the simplest problem for a single penny-shaped crack ($N = 1$) in an isotropic elastic medium subjected to a normal tensile load (well-known Sack’s problem). The solution of this problem can be found as a particular case of the solution for a single spheroidal cavity. First, for the prescribed constant loads at infinity the regular part of solution (1) has the form

$$\mathbf{U}_0 = \hat{\mathbf{E}} \cdot \mathbf{r}_1 = \sum_{i=1}^3 \sum_{t=0}^2 \sum_{s=-t}^t a_{is}^{(i)} \mathbf{s}_{is}^{(i)}(\mathbf{r}_1, f_1) \tag{3}$$

where $\hat{\mathbf{E}}$ is a constant remote strain tensor and the coefficients $a_{is}^{(i)}$ have the values

$$\begin{aligned}
 a_{00}^{(3)} &= \frac{f_1}{2\nu_0 - 1}(E_{11} + E_{22} + E_{33}), & a_{20}^{(1)} &= \frac{f_1}{3}(2E_{33} - E_{11} - E_{22}) \\
 a_{21}^{(1)} &= -\overline{a_{2,-1}^{(1)}} = f_1(E_{13} - iE_{23}), & a_{22}^{(1)} &= \overline{a_{2,-2}^{(1)}} = f_1(E_{11} - E_{22} - 2iE_{12})
 \end{aligned} \quad (4)$$

all other $a_{is}^{(t)}$ are equal to zero; ν_0 is the Poisson's ratio of the matrix material.

To find the unknowns $A_{is}^{(t)(1)}$ in the second part of eqn (2), we should substitute it into the boundary condition

$$\mathbf{T}_\xi(\mathbf{u}^{(0)})|_{\xi_1 = \xi_1^{(0)} = 0} = 0 \quad (5)$$

meaning that the crack's surface is stress-free. In eqn (5)

$$\mathbf{T}_\xi = \sigma_\xi \mathbf{e}_\xi + \tau_{\xi\eta} \mathbf{e}_\eta + \tau_{\xi\phi} \mathbf{e}_\phi$$

is a surface normal stress vector; in the limiting case $\xi_1^{(0)} = 0$ we have

$$\mathbf{T}_\xi = \mathbf{T}_z = \tau_{xz} \mathbf{e}_x + \tau_{yz} \mathbf{e}_y + \sigma_z \mathbf{e}_z.$$

The solution procedure is quite analogous to that described by Kushch (1996) and gives us the set of six linear algebraic equations ($t = 1$), that can be written in a matrix mode as

$$TG_t(\nu_0) \cdot \mathbf{A}_t + TM_t(\nu_0) \cdot \mathbf{a}_t = 0 \quad (6)$$

where the vector \mathbf{A}_t includes the unknowns $A_{i+2-i,s}^{(t)}$ and the vector \mathbf{a}_t includes the values $a_{i+2-i,s}^{(t)}$. The matrices TG_t and TM_t are defined by Kushch (1996); note only that in the case $\xi_1^{(0)} = 0$, considered by us, their expressions are simplified greatly.

The solutions (1)–(6) allow us to determine the stressed state of a medium with a penny-shaped crack for any constant remote load. So, for uniaxial tension $S_{33}/2\mu_0 = 1$ where S_{ij} are the components of the remote stress tensor \mathcal{S} and μ_0 is the shear modulus of a solid, we have only two non-zero coefficients $A_{is}^{(t)(1)}$: they are

$$A_{00}^{(1)(1)} = \frac{2}{3} \frac{1 + \nu_0}{\pi}; \quad A_{20}^{(3)(1)} = -\frac{1}{\pi}.$$

It is easy to show in this special case that the solution is equivalent to those obtained by Sack (1946), Sneddon (1946), Lure (1964) and others. Note, however, that the solutions (1)–(2) are valid also when an arbitrary variable external load, satisfied by an equilibrium condition, is prescribed. In this case the series expansion (3) of the regular part of solution \mathbf{U}_0 contains more (in principle, up to infinity) non-zero coefficients $a_{is}^{(t)}$, and, hence, the algebraic set (6) will contain equations with $t > 1$ as well.

When a medium contains a number $N > 1$ of cracks or inclusions placed so that their interaction cannot be neglected, the general solution procedure for a many-particle model should be used. In this case, in order to satisfy boundary conditions of type (5) on each crack or cavity and continuity conditions on the matrix–inclusion interfaces

$$[\mathbf{u}^{(0)} - \mathbf{u}^{(p)}]|_{\xi_p = \xi_p^{(0)} = 0} = 0; \quad [\mathbf{T}_{\xi_p}(\mathbf{u}^{(0)}) - \mathbf{T}_{\xi_p}(\mathbf{u}^{(p)})]|_{\xi_p = \xi_p^{(0)} = 0} = 0 \quad (7)$$

where $\mathbf{u}^{(p)}$ is the displacement vector within the p th inclusion, we should first transform eqns (1)–(2) to a p th local spheroidal basis and then substitute it into corresponding boundary conditions. Such a transformation is based on the addition theorems for the external partial solutions $S_{is}^{(t)}$ derived by Kushch (1995) and gives us the representation of $\mathbf{u}^{(0)}$ in the p th local spheroidal basis

$$\mathbf{u}^{(0)} = \sum_{i=1}^3 \sum_{l=0}^{\infty} \sum_{s=-l}^l [a_{is}^{(0)(p)} \mathbf{s}_{is}^{(0)}(\mathbf{r}_p, f_p) + A_{is}^{(0)(p)} \mathbf{S}_{is}^{(0)}(\mathbf{r}_p, f_p)]. \quad (8)$$

The solution procedure is described in detail by Kushch (1996) and Kushch (1998). As a result, we lead again to an infinite set of linear algebraic equations. In practice, only a finite sized algebraic set can be tackled numerically. However, when the number of equations [or, equivalently, the number of terms retained in the series (2)] is increased we approximate the exact solution more and more closely, in principle, with any desirable accuracy. The series (1)–(2), representing a displacement vector, converges in all points of the multiply-connected domain, a convergence rate of the series for the stresses is satisfactory everywhere except a small vicinity of crack’s tips, where some components of the stress tensor tend to infinity.

3. EXPRESSION FOR THE OPENING MODE STRESS INTENSITY FACTOR K_{IC}

It is a well known fact that the stress field produced by a crack has a singularity. So, for a solid containing a single penny-shaped crack in a plane $z = 0$ and subjected to the normal tensile load S_{33} , the expression of the normal stress σ_{zz} in the crack plane is $\sigma_{zz} = 0$ on the crack’s surface and

$$\sigma_{zz} = \frac{2S_{33}}{\pi} \frac{1}{\xi} \quad (9)$$

outside the crack (e.g. Lure, 1964). Due to axial symmetry of the problem, this expression is independent of the angle variable ϕ . It is clear that for $\rho = \sqrt{x^2 + y^2} \rightarrow f+0$, or, equivalently, for $\xi \rightarrow 0$ the stress σ_{zz} tends to infinity. The coefficient of the singular term $1/\xi$, normalised by the value $\sqrt{\pi f}$ is, by definition, the opening-mode stress intensity factor (SIF) K_{IC} that plays an important role in fracture mechanics. So, for a single penny-shaped crack we have the constant value $K_{IC} = 2\sqrt{f/\pi} S_{33}$.

On the other hand, when the crack is influenced by the disturbance field of another adjacent crack or inclusion, the SIF is no longer constant and may vary over a wide range depending on the structure parameters and the material properties. To find an expression for K_{IC} for the general solution of the many-particle model we should carry out an asymptotic analysis of the stress field related to the displacement field (1)–(2).

We begin with the analysis of the strains

$$\varepsilon_{ij} = \frac{1}{2}(u_{i,j} + u_{j,i}) \quad (10)$$

where

$$u_{i,j} = \frac{\partial u_i}{\partial x_j} = \frac{\partial u_i}{\partial \alpha_k} \frac{\partial \alpha_k}{\partial x_j} \quad \text{and} \quad u_i \quad (i = 1, 2, 3)$$

are the Cartesian components of the displacement vector \mathbf{u} . Here x_j ($j = 1, 2, 3$) are the Cartesian variables x , y and z whereas α_k ($k = 1, 2, 3$) are the oblate spheroidal variables ξ , η and ϕ , respectively. The matrix $J = \{\Psi_{kj}\} = \{\partial \alpha_k / \partial x_j\}$ has the form

$$J = \begin{Bmatrix} x\xi(h/f)^2 & y\xi(h/f)^2 & z\xi^2/\xi(h/f)^2 \\ -x\eta(h/f)^2 & -y\eta(h/f)^2 & z\eta^2/\eta(h/f)^2 \\ -y/(x^2 + y^2) & x/(x^2 + y^2) & 0 \end{Bmatrix} \quad (11)$$

where $h^2 = (\xi^2 + \eta^2)^{-1}$.

We are interested in the asymptotic behavior of the Ψ_{ij} as $\xi \rightarrow 0$. Taking into account that $h^2 \rightarrow 1/\eta^2 \neq 0$ for $\eta \neq 0$ we have the finite limiting values of all components of J . On

the other hand, for the value $\eta = 0$, associated with the crack's plane, $h^2 = 1/\bar{\xi}^2$ and we find that

$$\begin{aligned}\Psi_{11} &= \frac{1}{f^2} \frac{x}{\bar{\xi}} = \frac{1}{f} \frac{\xi}{\bar{\xi}} \cos \phi, & \Psi_{12} &= \frac{1}{f} \frac{\xi}{\bar{\xi}} \sin \phi, & \Psi_{13} &= \eta \left(\frac{\xi}{\bar{\xi}} \right)^2 = 0 \\ \Psi_{21} &= -x\eta(h/f)^2 = 0, & \Psi_{22} &= -y\eta(h/f)^2 = 0, & \Psi_{23} &= 1/(f\bar{\xi}) \\ \Psi_{31} &= -\sin \phi, & \Psi_{32} &= \cos \phi, & \Psi_{33} &= 0.\end{aligned}\quad (12)$$

Thus, the singular multiplier enters into the expressions for Ψ_{11} , Ψ_{22} and Ψ_{23} ; the rest of the Ψ_{ij} have finite or zero values at $\eta = 0$ and $\bar{\xi} \rightarrow 0$.

Now we observe that to evaluate the asymptotic behavior of the stress

$$\sigma_{zz} = 2\mu_0 \left(\varepsilon_{zz} + \frac{\nu_0}{1-2\nu_0} \nabla \cdot \mathbf{u} \right) \quad (13)$$

near the crack tip we need to perform this analysis for $\nabla \cdot \mathbf{u}$ and $\varepsilon_{zz} = \partial u_z / \partial z$ only. As to ε_{33} , we find easily from eqns (10) and (12) that

$$\varepsilon_{33} \Big|_{z=0} = \frac{1}{f\bar{\xi}} \frac{\partial u_z}{\partial \eta} \Big|_{\eta=0}. \quad (14)$$

Taking into account the representation of the displacement vector given by the series (8) we find that calculation of the partial derivative is reduced to calculation of this derivative from the partial solutions $\mathbf{s}_{ts}^{(i)}$ and $\mathbf{S}_{ts}^{(i)}$. To find them it is enough to use the explicit expressions of these functions and the limiting values of the associated Legendre's polynomials $P_i^j(i\bar{\xi})$ and $Q_i^j(i\bar{\xi})$ at $\bar{\xi} \rightarrow 0$.

So, for the internal solutions $\mathbf{s}_{ts}^{(i)}$ we have

$$\lim_{\bar{\xi} \rightarrow 0} \frac{\partial \mathbf{s}_{ts}^{(i)}}{\partial \eta} \Big|_{z=0} = 0, \quad i = 1, 2, 3; \quad t = 0, 1, 2, \dots; \quad |s| \leq t. \quad (15)$$

This result is expected because the internal solutions represent the regular part of solution. For the external (singular) solutions $\mathbf{S}_{ts}^{(i)}$ we find

$$\begin{aligned}\lim_{\bar{\xi} \rightarrow 0} \frac{\partial \mathbf{S}_{ts}^{(1)}}{\partial \eta} \Big|_{z=0} \cdot \mathbf{e}_z &= \begin{cases} (-1)^{(t+s)/2} \exp(is\phi) & \text{for } (t-s) \text{ even;} \\ 0 & \text{for } (t-s) \text{ odd;} \end{cases} \\ \lim_{\bar{\xi} \rightarrow 0} \frac{\partial \mathbf{S}_{ts}^{(2)}}{\partial \eta} \Big|_{z=0} \cdot \mathbf{e}_z &= \begin{cases} (-1)^{(t+s-1)/2} \frac{s}{t} \exp(is\phi) & \text{for } (t-s) \text{ odd;} \\ 0 & \text{for } (t-s) \text{ even;} \end{cases} \\ \lim_{\bar{\xi} \rightarrow 0} \frac{\partial \mathbf{S}_{ts}^{(3)}}{\partial \eta} \Big|_{z=0} \cdot \mathbf{e}_z &= \begin{cases} (-1)^{(t+s)/2} \left[\frac{4(1-\nu)-t}{t(2t-1)} (t^2-s^2) - 1 \right] \exp(is\phi) & \text{for } (t-s) \text{ even;} \\ 0 & \text{for } (t-s) \text{ odd.} \end{cases}\end{aligned}\quad (16)$$

To calculate $\nabla \cdot \mathbf{u}$ we use the properties of the partial solutions $\mathbf{s}_{ts}^{(i)}$ and $\mathbf{S}_{ts}^{(i)}$ with respect to differential operators derived by Kushch (1995). In particular, these functions are built so that

$$\nabla \cdot \mathbf{s}_{is}^{(1)} = \nabla \cdot \mathbf{s}_{is}^{(2)} = 0, \quad \nabla \cdot \mathbf{s}_{is}^{(3)} = 2(2\nu - 1) \frac{\partial}{\partial z} f_{i+1}^s, \quad (17)$$

where

$$f_i^s = \frac{(t-s)!}{(t+s)!} P_i^s(i\bar{\xi}) P_i^s(\eta) \exp(is\phi)$$

are the internal spheroidal harmonics. As it is easy to show, the derivative $\partial f_{i+1}^s / \partial z$ has a finite limiting value of $\bar{\xi} \rightarrow 0$ for arbitrary values of indices t and s .

Analogously, for the external solutions we have

$$\nabla \cdot \mathbf{S}_{is}^{(1)} = \nabla \cdot \mathbf{S}_{is}^{(2)} = 0, \quad \nabla \cdot \mathbf{S}_{is}^{(3)} = 2(2\nu - 1) \frac{\partial}{\partial z} F_{i-1}^s \quad (18)$$

where

$$F_i^s = \frac{(t-s)!}{(t+s)!} Q_i^s(i\bar{\xi}) P_i^s(\eta) \exp(is\phi)$$

are the external spheroidal harmonics. With the use of expressions (11) and (12) we find that

$$\lim_{\bar{\xi} \rightarrow 0} \bar{\xi} \nabla \cdot \mathbf{S}_{is}^{(3)} \Big|_{z=0} = \begin{cases} 2(2\nu - 1)(-1)^{(t+s)/2} \exp(is\phi) & \text{for } (t-s) \text{ even;} \\ 0 & \text{for } (t-s) \text{ odd;} \end{cases} \quad t \geq 2. \quad (19)$$

Summarising all of the above results and taking into account eqn (8) we find the expression for the opening-mode SIF for the p th crack:

$$\frac{1}{2\mu_0} K_{IC}^{(p)}(\phi_p) = \sqrt{f_p} \pi \lim_{\bar{\xi}_p \rightarrow 0} \bar{\xi}_p \frac{\sigma_{zz}}{2\mu_0} = \sqrt{\frac{\pi}{f_p}} \sum_{t=0}^{\infty} \sum'_{s=-t}^t (-1)^{(t+s)/2} \left\{ A_{is}^{(1)(p)} + \frac{2}{t+1} A_{i+1,s}^{(2)(p)} + \left[\frac{4(1-\nu)}{t(2t-1)} - 1 + 2\nu_0 \right] A_{is}^{(3)(p)} \right\} \exp(is\phi_p) \quad (20)$$

where the prime over the internal sum means that it contains only the terms with $(s-t)$ even.

Note that in a general case of arbitrarily placed and oriented cracks and inclusions in a solid subjected to a complex type loading not only σ_{zz} , but also other components of the stress tensor tend to infinity as $\bar{\xi} \rightarrow 0$. The corresponding shear-mode SIFs K_{IIC} and K_{IIIC} as well as the interacting energy and other parameters used in fracture mechanics can be calculated by analogy with K_{IC} using the results of the above asymptotic analysis. Our primary goal is, however, to show that the theory developed can be applied to effectively solve problems of interacting cracks and inclusions. The numerical results presented in the subsequent section allow an estimation of the potential abilities and the computational efficiency of the proposed method.

4. CALCULATION OF K_{IC} FOR A CRACK INTERACTING WITH ANOTHER CRACK OR INCLUSION

We begin our numerical analysis with the following simplest problem of the given class. So, we consider an elastic medium that contains two coplanar penny-shaped cracks

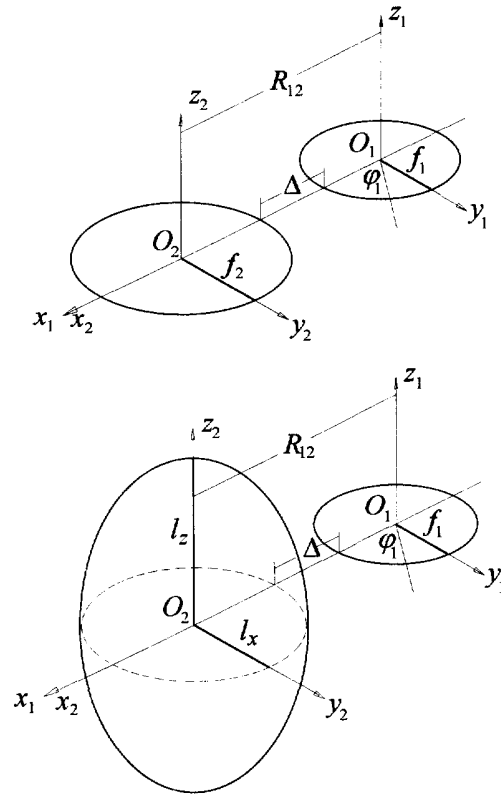


Fig. 2. (a) Sample problem geometry for crack-crack pair interaction ; (b) sample problem geometry for crack-inclusion pair interaction.

in a plane $z = 0$ (Fig. 2a). The remote load is uniaxial tension along the Oz -axis. When the cracks are widely separated, each of them can be considered independently as a single crack in an unbounded medium. However, when the cracks are drawn together, their interaction becomes more and more significant resulting in a local increase of K_{IC} in the area of the circular crack boundary nearest to another crack. In this case the solution is represented by the infinite series (2) and its convergence is governed by the geometrical parameters of the problem under consideration.

The accuracy of the numerical solution is pre-determined by the maximum value of index t retained in the computer realisation of the algorithm. It is possible to estimate the convergence rate of the series (20) and the accuracy of the numerical results presented below from Table 1, where the maximum values of the dimensionless SIF $K_{IC}^* = \max(K_{IC}^{(t)}/K_{IC}^c)$ are given calculated from the problem of two equal cracks $f_1 = f_2$ with the various maximum values of index $t = t_{\max}$. The $\max K_{IC}$ is of particular interest for us because this

Table 1. Convergence of the $K_{IC}^* = \max(K_{IC}^{(t)}/K_{IC}^c)$ with t_{\max} increased in the problem on two equal coplanar cracks $f_1 = f_2$

t_{\max}	Δ/f_1				
	0.5	0.2	0.1	0.05	0.02
1	1.020	1.035	1.046	1.054	1.060
3	1.052	1.114	1.166	1.211	1.253
5	1.061	1.153	1.243	1.333	1.430
7	1.064	1.168	1.283	1.410	1.563
9	1.064	1.174	1.302	1.455	1.658
11	1.064	1.176	1.311	1.482	1.726
13	1.064	1.177	1.315	1.497	1.774
15	1.064	1.177	1.317	1.506	1.808

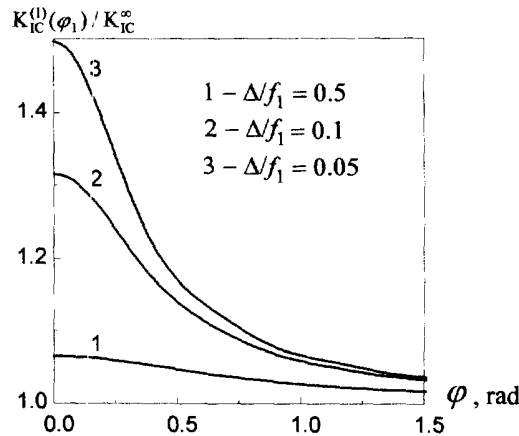


Fig. 3. Dimensionless SIF $K_{IC}^{(1)}(\phi_1)/K_{IC}^\infty$ variation along the boundary of 1st crack in the problem for two equal coplanar cracks: (line 1) $\Delta/f_1 = 0.5$; (line 2) $\Delta/f_1 = 0.1$; (line 3) $\Delta/f_1 = 0.05$.

is a factor controlling propagation of a crack. Here K_{IC}^∞ is the value of the SIF for a single crack, $\Delta = R_{12} - (f_1 + f_2)$ is the distance between the cracks and R_{12} is the distance between the centres of cracks (Fig. 2a). An analysis of Table 1 shows that the convergence rate of the solution is strongly governed by the parameter Δ/f_1 . We see also that the convergence with t_{max} increased is rapid enough and that for only the very closely placed cracks $\Delta/f_1 \leq 0.02$ the value $t_{max} = 15$ is insufficient and the additional terms in the series (1) should be taken into account.

The value $t_{max} = 15$ was adopted for the subsequent calculations, since Table 1 shows that K_{IC} is evaluated with relative error less than 1% for $\Delta/f_1 \geq 0.05$. Note, that at $\phi = 0$, chosen for the calculations (here SIF has a maximum), the convergence rate has a minimum; for the rest of the points on the crack's boundary the series (20) converges faster resulting in increased accuracy of calculations. The problem for two equal coplanar penny-shaped cracks was considered already by other authors; however, they present the numerical results only for cracks separated by a relatively large distance. The values presented in Table 1 agree with the value $K_{IC}^* = 1.065$ reported by O'Donoghue *et al.* (1985) for $\Delta/f_1 = 0.5$ and visually coincide with the plotted data by Kit and Hay (1989) for $\Delta/f_1 \geq 0.2$, but differ from the data by Xiao *et al.* (1994) where the equivalent inclusion method was applied and only a few first terms in a series expansion of K_{IC} , obtained by applying the superposition process, are taken into account.

As mentioned above, the SIF, due to interaction effects, is no longer constant on the crack boundary $r_1 = f_1$. The plots in Fig. 3 illustrate the local behavior of K_{IC} in the zone of the crack boundary nearest to another crack, $|\phi_1| \leq \pi/2$. It is seen from plots that as $\Delta/f_2 \rightarrow 0$ the non-uniformity of K_{IC} and its maximum value increases greatly. On the opposite side of the crack ($|\phi_1| > \pi/2$) the SIF has practically the same value as for a single crack.

In the examples presented above we had two equally sized cracks with identical values of K_{IC}^* on both cracks. However, for two unequal ($f_1 \neq f_2$) cracks we have $K_{IC}^{*(1)} \neq K_{IC}^{*(2)}$. Their values as the functions of the ratios $f_2/f_1 \geq 1$ and Δ/f_1 are given in Tables 2 and 3,

Table 2. Dimensionless SIF $K_{IC}^* = \max(K_{IC}^{(1)}/K_{IC}^\infty)$ on the 1st crack as a function of Δ/f_1 and f_2/f_1

f_2/f_1	Δ/f_1			
	0.5	0.2	0.1	0.05
1.0	1.064	1.18	1.32	1.51
1.5	1.116	1.28	1.47	1.72
2.0	1.169	1.38	1.61	1.90
2.5	1.224	1.47	1.74	2.06
3.0	1.276	1.56	1.86	2.22

Table 3. Dimensionless SIF $K_{IC}^* = \max(K_{IC}^{(1)}/K_{IC}^\infty)$ on the 2nd crack as a function of Δ/f_1 and f_2/f_1

f_2/f_1	Δ/f_1			
	0.5	0.2	0.1	0.05
1.0	1.064	1.18	1.32	1.51
1.5	1.058	1.16	1.28	1.45
2.0	1.049	1.15	1.26	1.40
2.5	1.047	1.14	1.24	1.37
3.0	1.046	1.13	1.23	1.34

respectively. It is seen from these tables that the maximum value of SIF is always greater on the smaller, say 1st, crack and it grows monotonically as the ratio f_2/f_1 is increased. Note, that the analogous data for the case $f_2/f_2 < 1$ are also available from these tables by renumeraling the cracks.

It is of particular interest to investigate the interactions between cracks and inclusions or cavities because these data can provide insight into understanding the nature of the strengthening effect produced by the hard particles of disperse phase of a composite. Consider a penny-shaped crack of radius f_1 and a spheroidal inclusion placed so as shown in Fig. 2(b). The shape parameter of the spheroid is $\varepsilon_2 = l_z/l_x$, where l_x and l_z are the spheroid's semiaxes along the axes Ox and Oz , respectively. For the purpose of convenient comparison we require that the volume of the inclusion $V_2 = \frac{4}{3}\pi l_x l_y l_z = \frac{4}{3}\pi (f_1)^3$ is constant. In particular, for the case $l_x = l_z$ (spherical inclusion) we set the radius of the sphere $R_2 = f_1$.

The lines 1–3 in Fig. 4 demonstrate the behavior of the dimensionless SIF K_{IC} near the hard ($\mu_2 = 1000 \mu_0$) inclusion. Calculations are performed for $\Delta/f_1 = 0.05$, where Δ here is the distance between the crack and the surface of spheroid (Fig. 2b). It is seen from the plots in Fig. 4 that the hard inclusion decreases greatly the SIF in the zone of the crack boundary nearest to inclusion and, thus, inhibits the crack propagation. Calculations show also that the strengthening effect of the elongated particles, in particular, the short fibres (line 1), is greater than that of the oblate spheroids.

On the other hand, the cavities produce a considerable increase of the K_{IC}^* values and, therefore, the risk of rupture (Fig. 5). The calculations show that the K_{IC} variation is governed mainly by the shape parameter ε_2 of the inhomogeneity of constant volume V_2 , by its shear moduli μ_2 and by the relative distance between the crack and inclusion, Δ/f_1 . Some results of the parametric study of this problem are given in Table 4.

Finally, the data in Table 5 demonstrate how the particle's size affects the K_{IC}^* . The form of inhomogeneity is assumed to be spherical. The calculations were made for the particles with radius $R_2 = 0.5f_1$ and $R_2 = 2f_1$; the data for $R_2 = f_1$ are contained in the

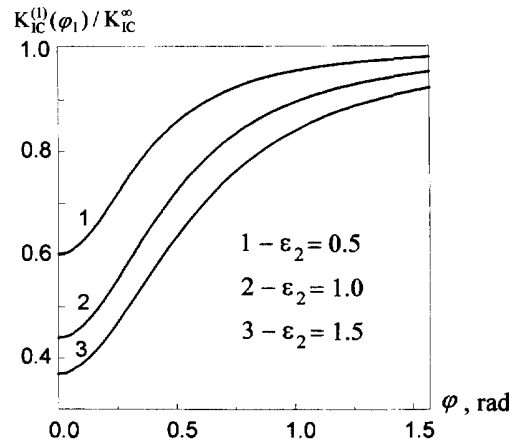


Fig. 4. Dimensionless SIF $K_{IC}^{(1)}(\phi_1)/K_{IC}^\infty$ variation along the boundary of the crack due to the nearby hard inclusion, of constant volume: (line 1) $\varepsilon_2 = 0.5$; (line 2) $\varepsilon_2 = 1.0$; (line 3) $\varepsilon_2 = 1.5$.

Table 4. Dimensionless SIF $(K_{IC}^{(1)}/K_{IC}^{\infty})|_{\phi=0}$ on the crack near the spheroidal inclusion of constant volume as a function of ε_2 , Δ/f_1 and μ_2/μ_0

ε_2	μ_2/μ_0	Δ/f_1			
		0.5	0.2	0.1	0.05
0.5	0	1.116	1.32	1.55	1.79
	10	0.963	0.88	0.78	0.67
	1000	0.958	0.86	0.74	0.60
1.0	0	1.110	1.28	1.43	1.58
	10	0.914	0.77	0.65	0.54
	1000	0.895	0.72	0.56	0.43
1.5	0	1.103	1.24	1.35	1.47
	10	0.873	0.71	0.59	0.50
	1000	0.836	0.63	0.48	0.37

Table 5. Dimensionless SIF $(K_{IC}^{(1)}/K_{IC}^{\infty})|_{\phi=0}$ on the crack near the spherical inclusion as a function of R_2/f_1 , Δ/f_1 and μ_2/μ_0

R_2/f_1	μ_2/μ_0	Δ/f_1			
		0.5	0.2	0.1	0.05
0.5	0	1.031	1.12	1.24	1.37
	0.5	1.010	1.04	1.08	1.12
	2	0.990	0.96	0.92	0.88
	10	0.977	0.90	0.80	0.68
	1000	0.972	0.88	0.75	0.61
2.0	0	1.273	1.50	1.66	1.82
	0.5	1.089	1.16	1.21	1.26
	2	0.911	0.84	0.79	0.75
	10	0.781	0.60	0.49	0.41
	1000	0.732	0.51	0.38	0.29

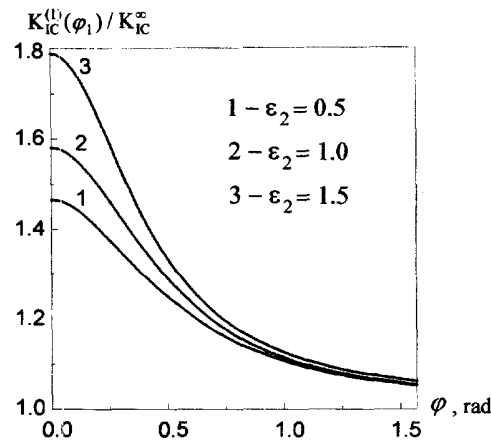


Fig. 5. Dimensionless SIF $K_{IC}^{(1)}(\phi_1)/K_{IC}^{\infty}$ variation along the boundary of the crack due to the nearby cavity of constant volume: (line 1) $\varepsilon_2 = 0.5$; (line 2) $\varepsilon_2 = 1.0$; (line 3) $\varepsilon_2 = 1.5$.

Table 4. It follows from the Table 5 that the larger is R_2/f_1 , the greater is the deviation of K_{IC}^* from unity. Note, that at $R_2 \ll f_1$ we approach the problem for the interacting inclusion and the half-plane crack whereas at $R_2 \gg f_1$ we lead to a problem for the penny-shaped crack near the interface of two dissimilar materials.

5. CONCLUDING REMARKS

As the results presented above of the numerical study show, the proposed rigorous analytical method of solution is efficient from a computational standpoint and provides high-accuracy analysis of the interaction between penny-shaped cracks and spheroidal inclusions. Although our attention was focused on the opening-mode stress intensity factor, the general analytical form of solution makes it possible to investigate by the same manner also the shear-mode stress intensity factors, the crack opening displacement, the interaction energy and other parameters commonly used in fracture mechanics. Only a few basic configurations were chosen here for the numerical analysis which illustrate the influence on the SIF of the structural parameters. However, the theory developed in the paper is applicable also to a cracked solid with a quasi-random distribution of cracks and to the particle composite with a cracked matrix. To this end the generalised structure model of a composite developed by Kushch (1997) can be used. In doing this, not only penny-shaped cracks, but also needle-like cracks can be considered. The only problem arising in this case is the stress analysis near the tip of the crack; it should be performed by analogy with the analysis described in Section 3 of this paper.

Acknowledgements—This work was made possible in part by Award #UE1-334 of the U.S. Civilian Research & Development Foundation for the Independent States of the Former Soviet Union (CRDF).

REFERENCES

- Andrejiv, A. E. (1982) *Spatial Problems in the Theory of Cracks*. Naukova Dumka, Kiev (in Russian).
- Collins, W. D. (1963) Some coplanar punch and crack problems in three-dimensional elastostatics. *Proceedings of the Royal Society of London* **A274**, 507–528.
- Fu, W. S. and Keer, L. H. (1969) Coplanar circular cracks under shear loading. *International Journal of Engineering Science* **7**, 361–374.
- Kit, G. S. and Hay, M. V. (1989) *Method of Potentials in the Three-dimensional Problems of Thermoelasticity for the Solids with Cracks*. Naukova Dumka, Kiev (in Russian).
- Kushch, V. I. (1995) Addition theorems for the partial vectorial solutions of Lamé's equation in a spheroidal basis. *International Journal of Applied Mechanics* **31**(2), 86–92.
- Kushch, V. I. (1996) Elastic equilibrium of a solid containing a finite number of aligned spheroidal inclusions. *International Journal of Solids and Structures* **33**, 1175–1189.
- Kushch, V. I. (1997) Microstresses and effective elastic moduli of a solid reinforced by periodically distributed spheroidal particles. *International Journal of Solids and Structures* **34**, 1353–1366.
- Kushch, V. I. (1998) Elastic equilibrium of a medium containing a finite number of arbitrary oriented spheroidal inclusions. *International Journal of Solids and Structures* **35**, 1187–1198.
- Lure, A. I. (1964) *Three-dimensional Problems of the Theory of Elasticity*. Wiley, New York.
- O'Donoghue, P. E., Nishioka, T. and Alturi, S. N. (1985) Multiple coplanar embedded elliptic cracks in an infinite solid subject to arbitrary crack force traction. *International Journal of Numerical Methods in Engineering* **21**, 437–449.
- Sack, R. A. (1946) Extension of Griffith's theory of rupture to three dimensions. *Proceedings of the Physics Society* **58**, 729–736.
- Sneddon, I. N. (1946) The distribution of stress in the neighbourhood of a crack in an elastic solid. *Proceedings of the Royal Society of London* **A187**, 229–260.
- Sneddon, I. N. (1966) *Mixed Boundary-value Problems in Potential Theory*. Wiley, New York.
- Xiao, Z. M., Lim, M. K. and Liew, K. M. (1994) Stress intensity factors for two coplanar penny-shaped cracks under uniaxial tension. *International Journal of Engineering Science* **32**, 303–311.